Memoirs of the Faculty of Engineering, Okayama University, Vol.24, No. 1, November 1989

Fundamental Study on Electrical Discharge Machining

Yoshiyuki UNO*, Toshikatsu NAKAJIMA* and Osamu ENDO*

(Received October 13 , 1989)

SYNOPSIS

The generation mechanism of crater in electrical discharge machining is analyzed with a single pulse discharge device for alloy tool steel, black alumina ceramics, cermet and cemented carbide, investigating the gap voltage, the discharge current, the shape of crater, the wear of electrode and so on.

The experimental analysis makes it clear that the shape of crater has a characteristic feature for the kind of workpiece. The shape of electrode, which changes with the wear by an electric spark, has a significant effect on the shape of crater. The diameter and the depth of crater have a close relation to the discharge energy for alloy tool steel, black alumina ceramics and cermet, while those for cemented carbide are related to the discharge current. The shape factor which is the ratio of the depth to the diameter of crater is different for the work material.

1. INTRODUCTION

Electrical discharge machining has recently been developed as an effective machining method for difficult to cut or grind materials. The phenomenon in electric discharge machining is very

* Department of Mechanical Engineering

complex and has not yet been made clear sufficiently, because it takes place by an electric spark occured in the presence of a dielectric fluid through very small gap between an electrode and a workpiece. Material removal in electrical discharge machining is performed as an assemblage of crater generated by electrical discharge between an electrode and a workpiece. A study on material removal mechanism should therefore be based on an analysis of a crater generated by a single pulse discharge.

In this paper, from the above point of view, a fundamental study of material removal mechanisms of alloy tool steel, black alumina ceramics, cermet and cemented carbide is made with a single pulse method, investigating the discharge current and voltage, the electrode wear, the size and shape of a crater generated on the workpiece, the spark gap between an electrode and a workpiece and so on.

2. EXPERIMENTAL PROCEDURE

2.1 Single Pulse Discharge Device

A schematic diagram of experimental apparatus of ram-type electrical discharge machining used in this study is shown in Fig.1. In this device, transistor-pulsed circuit is used as a power supply, the electrode descends gradually till an electric spark occurs under a certain gap voltage and the electrode ascends rapidly just after the spark. The discharge current detected with the current monitoring sensor and the discharge voltage are recorded in digital storage oscilloscope and they are hard-copied by a recorder. The spark gap is measured by detecting motion of ram with non-touching displacement sensor. The shape of crater generated by a single pulse discharge is measured with profile meter. An electrode and a crater are observed with microscope and scanning electron microscope. Polarity of electrode is set plus in this test.

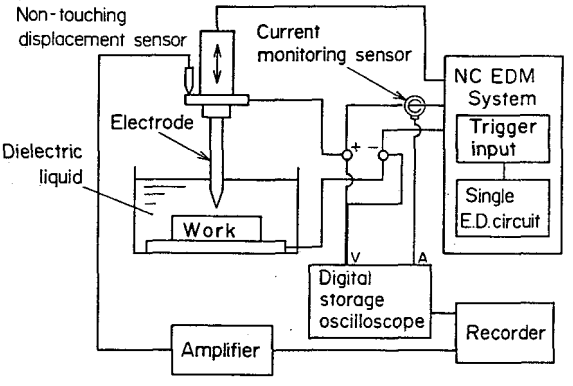

Fig.1 Schematic diagram of experimental apparatus with a single pulse discharge device

2.2 Electrode

Copper rod (Φ 10) is used as an electrode in this test. In order to prevent the effect of electrode wear[1], the shape of electrode is kept constant before each test except the test of electrode wear. As shown in the Fig.2, the electrode is shaped to be conical. The vertical angle is 40° (Fig.2(a)) and the nose radius is about 20μ m(Fig.2(b)).

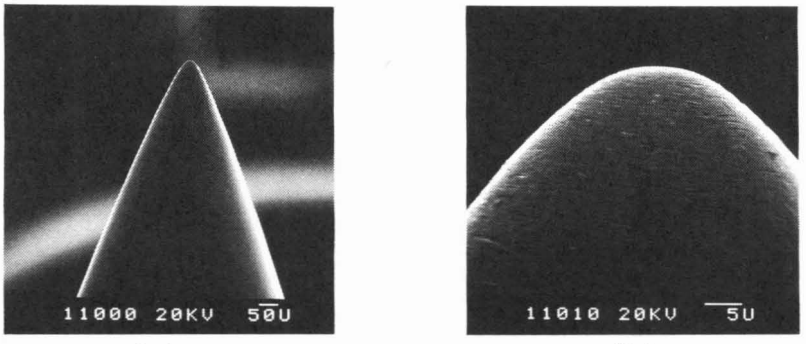

(a) (b)

Fig.2 SEM photographs of an electrode

2.3 Test Materials

Chemical composition and some mechanical properties of materials used as workpieces alloy tool steel SKD11, black alumina ceramics BA, cermet CM and cemented carbide CC are shown in Table 1. All workpieces are finished smoothly less than Ra = 0.03 μ m in surface roughness before the test. In the case of SKD11, it is ground with WA wheel and lapped with alumina powder, while metal bonded diamond wheel and diamond powder are used for other materials.

Table 1 Test materials

Material	Composition								Hardness Hv
SKD11	C	Si	Mn	P	S	Cr	Mo	V	670
	1.40	0.31	0.38	0.025	0.008	12.09	0.86	0.24	
	WC	TiC	Al_2O_3	Co	Ni	Bending Strength MPa			Hardness Hv
BA		30	70			900			1900
CM		79			21	1800			1300
CC	93			7		2200			1500

2.4 Test Condition of Electrical Discharge Machining

Fig.3 shows a measured example of variation of gap voltage and current between an electrode and a workpiece in a single pulse discharge. The electrode approaches gradually the workpiece under the setting voltage E_0. When the isolation of dielectric fluid is broken, an electric spark occurs. The gap voltage falls down to discharge voltage E_p and discharge current I_p appears simultaneously. Electrical discharge continues for presetting duration T_{ON}. After the period, both gap voltage and current become to zero. The discharge energy exhausted in a single pulse is expressed by;

$$\varepsilon = E_p \cdot I_p \cdot T_{ON} \quad ---- \quad (1)$$

In this study, the condition of electrical discharge machining is set as follows;
Setting voltage: E_0 =90V
Discharge current: I_p =14,26,38A
Discharge duration: T_{ON} =8-220μ s

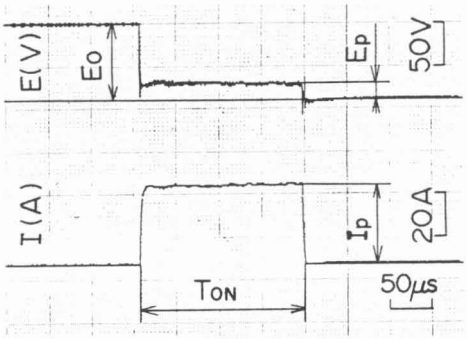

Fig.3 Variation of gap voltage and discharge current

3. ANALYSIS OF A CRATER GENERATED BY A SINGLE PULSE DISCHARGE

3.1 Observation of a Crater

Fig.4 is a SEM photogragh of a crater generated by a single pulse discharge on alloy tool steel and Fig.5 shows a schematic diagram of a crater. As shown in these figures, a crater is

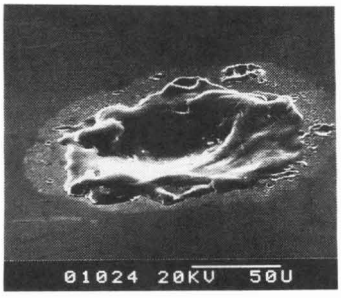

Fig.4 SEM photograph of a crater

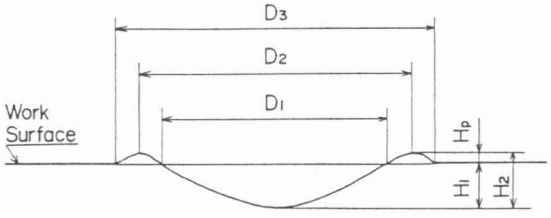

Fig.5 Schematic diagram of a crater

composed of a hollow part and a piled-up part around the hollow. It is considered that the material of a hollow part is melt or vaporized and blown off and the material of a piled-up part is resolidified after melting[2]. The shape of a crater is characterized by the following values shown in Fig.5.[3]

D_1 : Diameter of discharged crater

D_2 : Mean diameter of pile up

D_3 : Outside diameter of pile up

H_1 : Depth of discharged crater

H_p : Height of pile up

H_2 : Height from peak of pile up to valley of discharged crater

Among these values, diameter of discharged crater D_1 and depth of discharged crater H_1 are mainly used in the following analysis.

Figs.6(a)-(d) show micrographs and profiles of craters generated on alloy tool steel SKD11, black alumina ceramics BA, cermet CM, cemented carbide CC under the same machining condition respectively. As shown in these figures, each crater is composed of a hollow part at the center and a piled-up part around the hollow, but the size and the shape are greatly different for characteristics of workpiece. The depth of discharged crater H_1 becomes shallower in order of SKD11, BA, CM and CC, while the diameter of discharged crater D_1 becomes smaller in order of BA, SKD11, CM and CC. On the other hand, the height of pile up H_p for SKD11 is highest and becomes lower in order of CM, CC and BA. The pile up coefficient H_p/H_1 becomes higher in order of BA, SKD11, CM and CC. These values depend on the characteristics and electrical discharge machining ability of work material. The surfaces of crater on SKD11 and CM are very smooth and it is considered that these parts are melted and flowed. On the other hand, the surface of BA is irregular and height of pile up is very little as compared with that for other

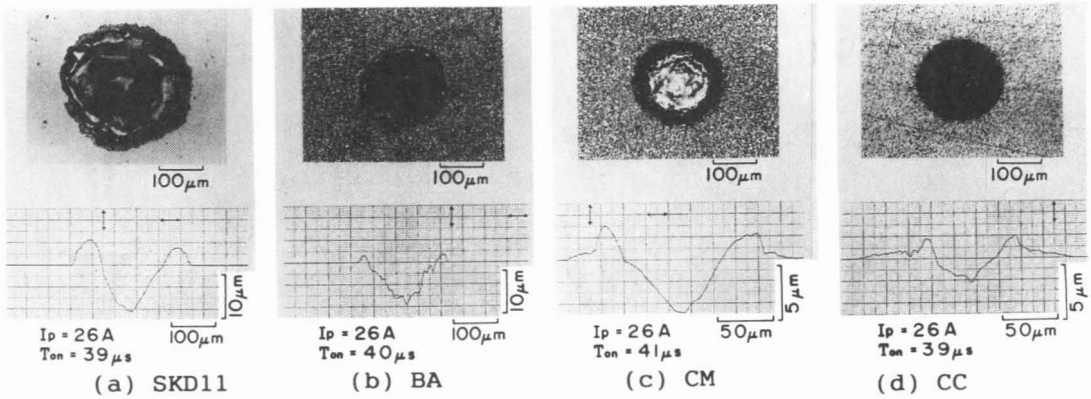

Fig.6 Micrographs and profiles of craters

materials. This means that abilities of melting and flowing for BA are not enough under this condition. Furthermore in the case of CC, the depth of crater is nearly equal to the height of pile up, and it means that the electrical discharge machining of CC is very difficult under this condition.

3.2 Effect of Electrode Wear on the Generation of Crater

In electrical discharge machining, not only workpiece but also electrode is removed simultaneously. In this section, effects of the electrode wear on the shape and size of crater generated by a single pulse discharge are investigated. In each test, three successive single pulse discharges are given for various workpieces under the same condition with a pre-setting formed electrode. The wear of electrode and the size and shape of crater are observed and measured by microscope and/or surface profile meter.

Fig.7 shows photographs of crater and electrode in each stage of test. From the figure, variation process of electrode wear and crater generated with the electrode are observed. The size of crater on SKD11 and BA decreases slightly with the wear of electrode. On the other hand, the size of center part where the material is melted for CM and CC decreases significantly with the wear of electrode, while the size of blackening part which is considered as the discharge column is approximately kept constant.

Fig.8 shows the variation of the depth of crater with the number of single pulse n. As shown in the figure, the degree of effect is different for the kind of workpiece. In the case of SKD11, the wear of electrode have a great effect on the depth of crater. The depths by the second and the third pulse are 77 % and

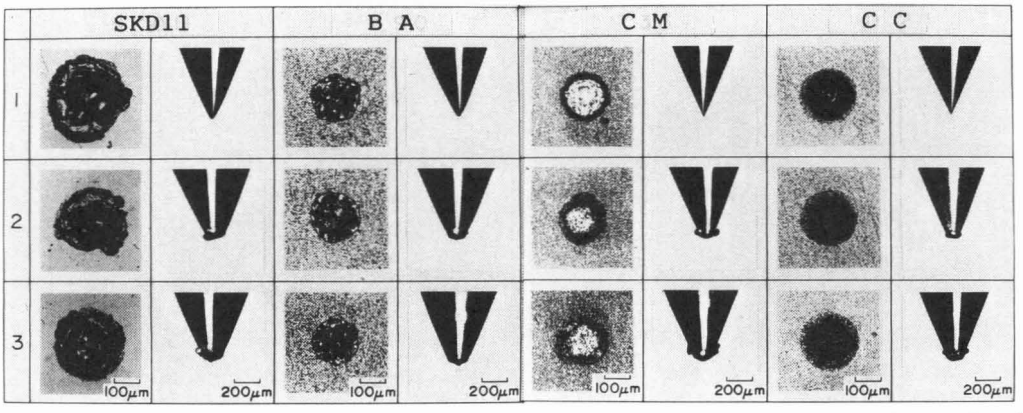

Fig.7 Photographs of crater and electrode in three successive single pulse discharge test for various kinds of workpieces

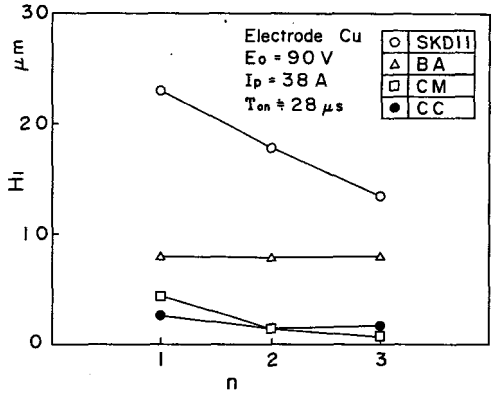

Fig.8 Variation of the depth of crater

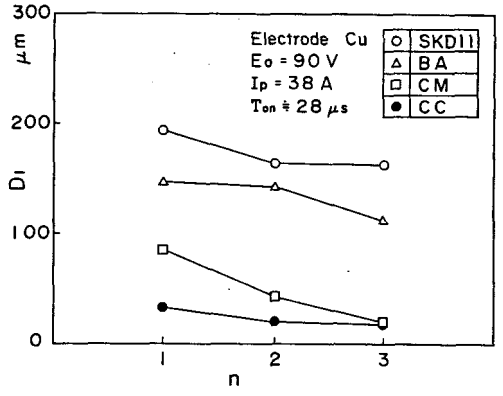

Fig.9 Variation of the diameter of crater

58 % of that by the first pulse respectively. On the other hand, the depth of crater in the case of BA is kept constant in spite of the electrode wear. In the cases of CM and CC, the depth of crater decreases with the wear of electode. Especially in the case of CM, the depths by the second and the third pulse decrease to the level of 33 % and 16 % respectively as compared with that by the first pulse. In the case of CC, the depth of crater by the third pulse is 62 % of that by the first pulse.

Fig.9 shows the variation of the diameter of crater D_1 with the number of single pulse n. As can be seen in the figure, D_1 decreases with the wear of electrode for all workpieces, the diameters by the third pulse are 80 % for SKD11, 77 % for BA, 25 % for CM and 56 % for CC of that by the first pulse. The decrease of diameter for CM is remarkable and similar to the case of the depth of crater H_1.

Fig.10 is the measured example of profile of crater in the successive single pulse discharges for cemented carbide CC. It can be seen that the size of crater becomes smaller and the surface becomes more irregular with the number of pulse. This is caused by the wear of electrode, which leads to the dispersion of pressure occured between an electrode and a workpiece.

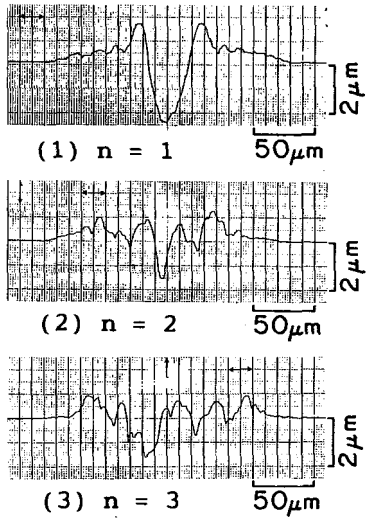

Fig 10 Variation of the shape of crater

3.3 Growth of Discharge Column

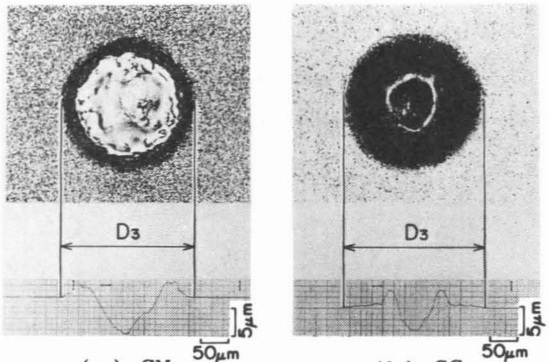

(a) CM (b) CC

Fig.11 Discharge column for CM and CC

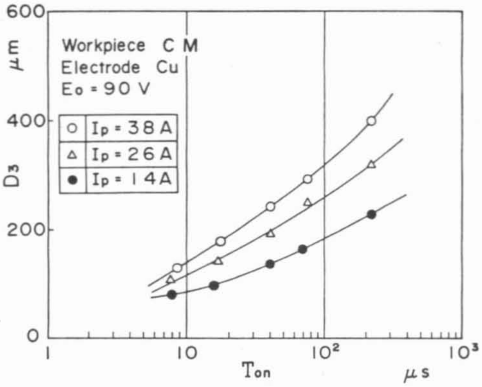

Fig.12 Relation between D_3 and T_{ON} for CM

As shown in Fig.11, the blackening part exists around the crater in the cases of CM and CC, which is considered to be discharge column. The surface of this part is irregular and the diameter of the part is equal to the diameter of pile up D_3.

Fig.12 shows the relations between the diameter of discharge column D_3 and discharge duration T_{ON} for CM with three kinds of discharge current I_p. As shown in the figure, the diameter of discharge column D_3 increases with discharge duration T_{ON} and discharge current I_p. The following experimental relation is reported[4] ;

$$D_3 = K \sqrt{T_{ON}} \quad \text{------------------} \quad (2)$$

where K is a constant depending on machining condition.
D_3 in this case increases following the equation (2) qualitatively. In the case of CC, D_3 has also the same relation to T_{ON}.

3.4 Effect of Machining Condition on the Shape of Crater

Fig.13 is a photograph which shows the shape of crater generated on various workpieces with three kinds of discharge duration T_{ON} under the setting voltage E_0 = 90V and the discharge current I_p = 38A. It should be noticed that all discoloured area is not equal to the size of crater as mentioned above.

Fig.14 shows the relations between the diameter of crater and the discharge duration T_{ON} for four kinds of workpieces. As shown in the figure, the diameter of crater becomes smaller in order of SKD11, BA, CM and CC under the same condition. In the case of SKD11 and BA, D_1 increases with increasing T_{ON}, and D_1 becomes about twice when T_{ON} increases by ten times. In the case of CM, on the

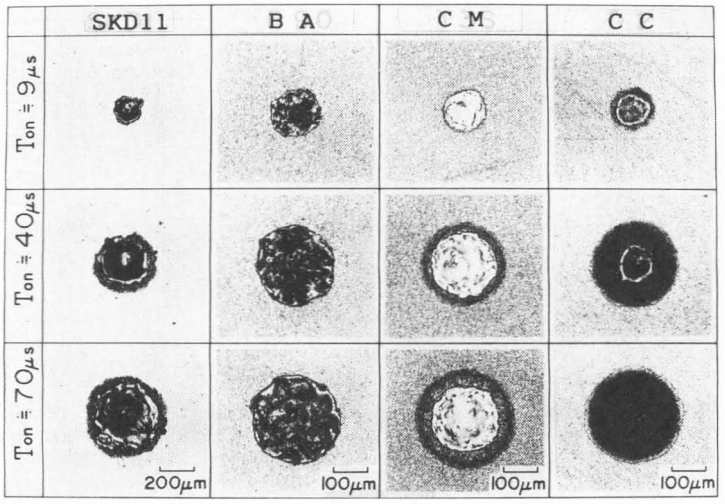

Fig.13 Photographs of craters on various kinds of workpieces

other hand, D_1 stops increasing where the discharge duration T_{ON} becomes over several scores of micro second. As observed in Fig.13, D_1 is approximately constant in the cases of T_{ON} = 40 μs and 70μs while D_3 increases with T_{ON}. From this fact, it should be noticed that the discharge duration T_{ON} for CM has a lower limit with increasing the diameter of crater. Furthermore D_1 for CC is nearly constant with an increase of T_{ON}. As shown in Fig.13, the crater is not observed clearly for long discharge duration.

Fig.15 shows the relations between the diameter of crater D_1 for SKD11 and the discharge energy ε with three kinds of discharge current I_p. As shown in the figure, D_1 increases with increasing ε and I_p. In the case of I_p = 14A, the rate of increase of D_1 is low as compared with those in the other cases.

Fig.16 shows the relations between the depth of crater H_1 and the discharge energy ε with three kinds of I_p. It can be seen that the relations are similar to those in Fig.15. Then the shape

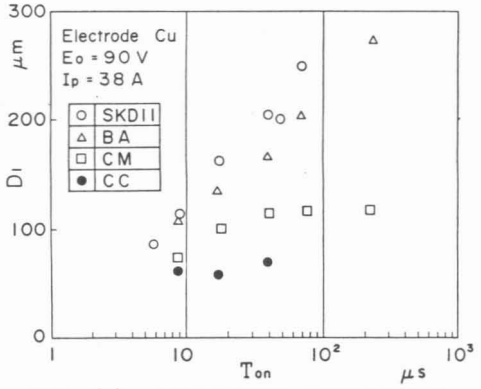

Fig.14 Relations between D_1 and T_{ON}

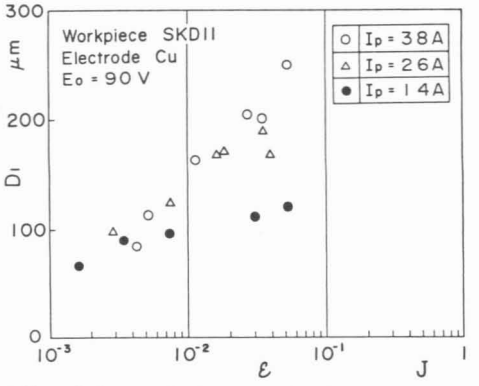

Fig.15 Relations between D_1 and ε for SKD11

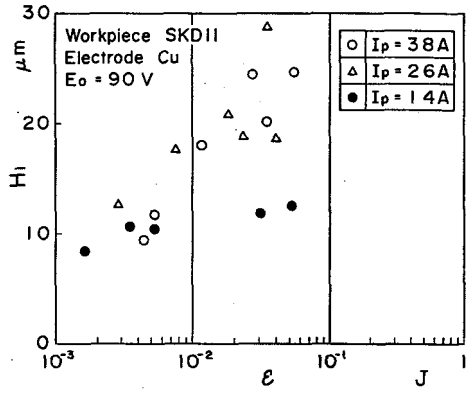

Fig.16 Relations between H_i and ε for SKD11 with three kinds of I_p

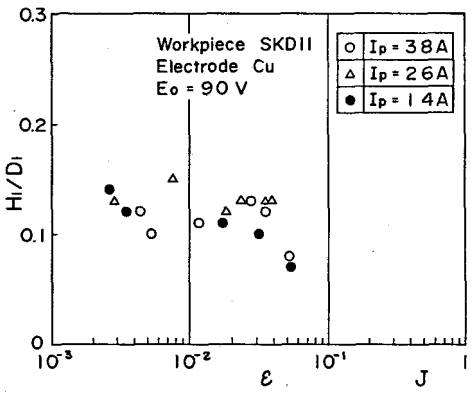

Fig.17 Relations between the shape factor H_i/D_i and ε for SKD11

factor, which is the ratio of the depth of crater to the diameter of crater, is introduced for analysis of the shape of crater.

Fig.17 shows the variation of the shape factor H_i/D_i with the discharge energy ε. As can be seen from the figure, the shape factor H_i/D_i is closely related to the discharge energy ε for various I_p. The value H_i/D_i is about 0.12 for small ε and becomes lower for larger ε. This indicates that larger heat energy pulse leads to shallower crater.

Fig.18 shows the relations between the diameter of crater D_i on black alumina ceramics BA and the discharge energy ε for three kinds of I_p. As shown in the figure, the diameter of crater D_i is closely related to the discharge energy ε for BA, and D_i increases with increasing ε. The depth of crater H_i has also the similar relation to the discharge energy ε.

Fig.19 shows the variation of the shape factor H_i/D_i with the discharge energy ε for BA. There is no relation between H_i/D_i and ε

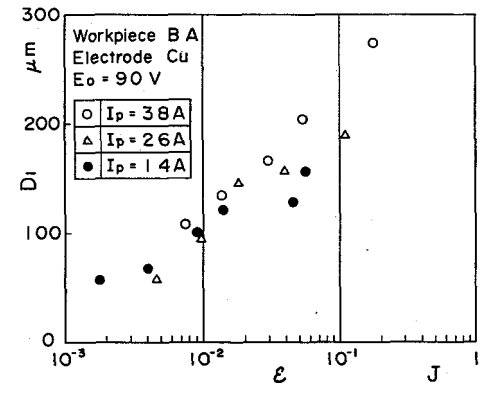

Fig.18 Relations between D_i and ε for BA with three kinds of I_p

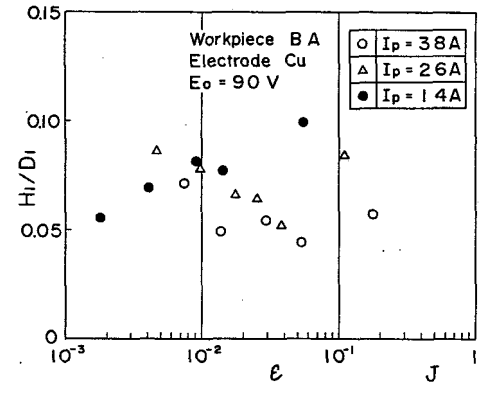

Fig.19 Relations between the shape factor H_i/D_i and ε for BA

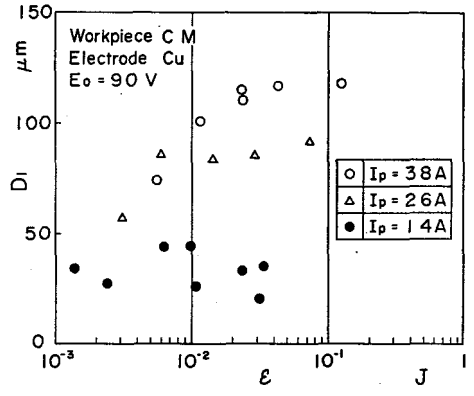

Fig.20 Relations between D_i and ε for CM with three kinds of I_p

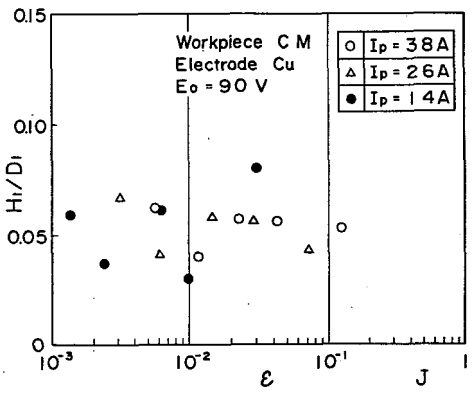

Fig.21 Relations between the shape factor H_i/D_i and ε for CM

in this case. The value of H_i/D_i is between 0.05 - 0.1, which is smaller as compared with that for SKD11.

Fig.20 shows the relations between the diameter of crater D_i for cermet CM and the discharge energy ε with three kinds of I_p. As shown in the figure, the diameter of crater D_i increases with increasing the discharge energy ε for I_p = 38A and 26A, while D_i is approximately constant for I_p = 14A. This means that the discharge current over a critical level is necessary for efficient machining in the case of CM.

Fig.21 shows the variation of the shape factor H_i/D_i with the discharge energy ε for CM. The value of H_i/D_i is about 0.05 for various discharge energy ε, which is smaller than that for BA.

Fig.22 shows the relations between the diameter of crater D_i for cemented carbide CC and the discharge energy ε with three kinds of I_p. As shown in the figure, the diameter of crater D_i is

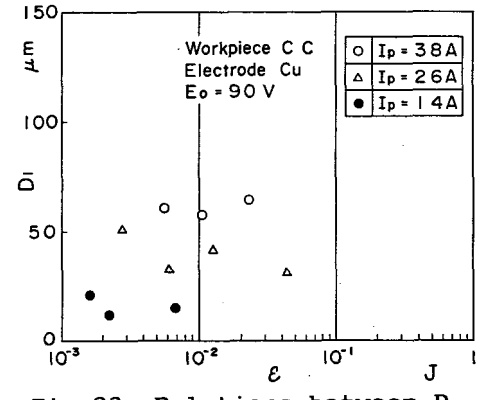

Fig.22 Relations between D_i and ε for CC with three kinds of I_p

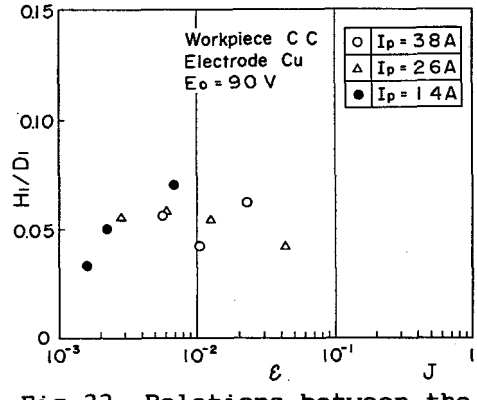

Fig.23 Relations between the shape factor H_i/D_i and ε for CC

approximately constant with the discharge energy ε, and higher discharge current leads to larger diameter of crater.

Fig.23 shows the variation of the shape factor H_1/D_1 with the discharge energy ε for CC. The value of H_1/D_1 is about 0.05 for various discharge energy ε, which is similar to that for CM.

4. CONCLUSIONS

Single pulse discharge test is carried out for fundamental analysis of electrical discharge machining. The generation mechanism of crater on workpiece is investigated by measuring of the shape of crater and observing the surface of crater and wear of electrode and so on. Main results obtained are as follows;

(1) The shape of crater is different and has characteristic feature for the kind of the workpiece respectively.

(2) The shape of electrode has a significant effect on the shape of crater. The sharper the electrode tip is, the bigger the crater becomes.

(3) The diameter of discharge column increases with increasing the discharge duration.

(4) The diameter and the depth of crater have a close relation to the discharge energy for alloy tool steel SKD11, black alumina ceramics and cermet, while those for cemented carbide are affected by the discharge current.

(5) The shape factor which is the ratio of the depth to the diameter of crater is different for the kind of workpiece, about 0.1 for alloy tool steel SKD11, 0.05-0.1 for black alumina ceramics, about 0.05 for cermet and cemented carbide.

REFERENCES

1) H.TSUCHIYA, H.GOTO and M.MIYAZAKI: A Basic Study on Electrical Discharge Machining, Journal of the Japan Society of Electrical Machining Engineers, 22, 43, (1988) 1.

2) J.R.CROOKALL and B.C.KHOR: Electro-Discharge Machined Surfaces, Proceedings of the 15th MTDR Conference (1975) 373.

3) K.INOUE: Principle of Electrical Discharge Machining, Society of Non-Traditional Technology (1979) 15.

4) ibid 3) 14.